Journal of Nuclear Medicine, published on December 21, 2017 as doi:10.2967/jnumed.117.204669

Intra-individual comparison of ^{18}F-PSMA-1007 and ^{18}F-DCFPyL PET/CT in the prospective evaluation of patients with newly diagnosed prostate carcinoma: A pilot study.

Frederik L. Giesel[1,2,†], Leon Will[1,†], Ismaheel Lawal[3], Thabo Lengana[3], Clemens Kratochwil[1], Mariza Vorster[3], Oliver Neels[4], Florette Reyneke[3], Uwe Haberkon[1,2], Klaus Kopka[4], and Mike Sathekge[3,*]

Affiliations

1 Department of Nuclear Medicine, Heidelberg University Hospital, Im Neuenheimer Feld 400, 69120 Heidelberg, Germany
2 Cooperation Unit Nuclear Medicine, German Cancer Research Center (DKFZ), Im Neuenheimer Feld 280, 69120 Heidelberg, Germany
3 Department of Nuclear medicine, University of Pretoria and Steve Biko Academic Hospital, Private Bag X169, Pretoria, 0001, South Africa
4 Division of Radiopharmaceutical Chemistry, German Cancer Research Center (DKFZ), Im Neuenheimer Feld 280, 69120 Heidelberg, Germany
† Contributed equally
* Corresponding author

Corresponding author:
Mike Sathekge, Department of Nuclear Medicine, University of Pretoria and Steve Biko Academic Hospital, Private Bag X169, Pretoria, 0001, South Africa. E-mail: mike.sathekge@up.ac.za

First authors:
Frederik L. Giesel, Department of Nuclear Medicine, Heidelberg University Hospital, Im Neuenheimer Feld 400, 69120 Heidelberg, Germany. Tel.: +49-6221-56-39461. E-mail: frederik@egiesel.com

Leon Will, Department of Nuclear Medicine, Heidelberg University Hospital, Im Neuenheimer Feld 400, 69120 Heidelberg, Germany. Tel.: +49-6221-56-7732. E-mail: leon.will@stud.uni-heidelberg.de (Medical student)

Disclaimer: Patent application for PSMA-1007 for FLG, KK and UH. The other authors declare that they have no conflict of interest.

Word count: 3.266 words

Running Title: Comparison of PSMA-1007 and DCFPyL

ABSTRACT

Introduction: The introduction of ^{18}F-labelled prostate-specific membrane antigen (PSMA) targeted positron emission tomography/computed-tomography (PET/CT) tracers, firstly ^{18}F-DCFPyL and more recently ^{18}F-PSMA-1007, have demonstrated promising results for the diagnostic workup of prostate cancer (PCa). This clinical study presents an intra-individual comparison to evaluate tracer-specific characteristics of ^{18}F-DCFPyL versus ^{18}F-PSMA-1007.

Methods: Twelve prostate cancer patients, drug naive or prior to surgery, received similar activities of about 250 MBq ^{18}F-DCFPyL and ^{18}F-PSMA-1007 48 h apart and were imaged 2 h p.i. in the same PET/CT-scanner using the same reconstruction-algorithm. Normal organ biodistribution and tumor uptakes were quantified using SUV_{max}.

Results: PSMA-positive lesions were detected in twelve out of twelve PCa patients. Both tracers, ^{18}F-DCFPyL and ^{18}F-PSMA-1007, detected the identical lesions. No statistical significance could be observed when comparing the SUV_{max} of ^{18}F-DCFPyL and ^{18}F-PSMA-1007 for local tumor, lymph node metastases and bone metastases. With regard to normal organs, ^{18}F-DCFPyL presented statistically significant higher uptake in kidneys, urinary bladder and lacrimal gland. Vice versa, significantly higher uptake of ^{18}F-PSMA-1007 in muscle, submandibular and sublingual gland, spleen, pancreas, liver and gallbladder was observed.

Conclusion: Excellent imaging quality was achieved with both ^{18}F-DCFPyL and ^{18}F-PSMA-1007 resulting in identical clinical findings for the evaluated routine situations. Non-urinary excretion of ^{18}F-PSMA-1007 might present some advantage with regard to delineation of local recurrence or pelvic lymph-node metastasis in selective patients; the lower hepatic background might favor ^{18}F-DCFPyL in very late stages when rare cases of liver metastases can occur.

Keywords: ^{18}F-PSMA-1007, ^{18}F-DCFPyL, Prostate carcinoma, PET/CT, PSMA

INTRODUCTION

Prostate-specific membrane antigen (PSMA) targeted positron emission tomography/computed-tomography (PET/CT) is a relatively new technique for imaging PCa. Initial results in the evaluation of various clinical indications, such as imaging guided biopsy, primary tumor staging, localisation of biochemical relapse, planning of radiotherapy, prediction and assessment of tumor response to systemic therapy are very promising and have been summarized in detail recently (*1-4*). Currently most clinical experience is available for the ligand Glu-urea-Lys(Ahx)-HBED-CC labelled with the generator radionuclide ^{68}Ga (^{68}Ga-PSMA-11). However, due to the promising clinical results it is predictable that the request for PSMA-PET/CT examinations will increase and the foreseeable quantitative demand promoted the development of ^{18}F-labeled ligands, using [^{18}F]fluoride, a radionuclide that can be produced and distributed in large-scale and with reasonable costs by a cyclotron.

After pre-clinical evaluation of several ^{18}F-labeled PSMA-ligands, (2-(3-{1-carboxy-5-[(6-^{18}F-fluoro-pyridine-3-carbonyl)-amino]-pentyl}-ureido)-pentanedioic acid) (^{18}F-DCFPyL) and (((3S,10S,14S)-1-(4-(((S)-4-carboxy-2-((S)-4-carboxy-2-(6-18F-fluoronicotinamido)butanamido)butanamido)methyl)phenyl)-3-(naphthalen-2-ylmethyl)-1,4,12-trioxo-2,5,11,13-tetraazahexadecane-10,14,16-tricarboxylic acid)) (^{18}F-PSMA-1007) were considered the most promising candidates (*5,6*) and have recently been introduced clinically (*7,8*). ^{18}F-DCFPyL already demonstrated non-inferiority versus ^{68}Ga-PSMA-11 in a one-on-one evaluation of 25 patients (*9*). Another 62 patients examined with ^{18}F-DCFPyL were found non-inferior to historical controls examined with ^{68}Ga-PSMA-11 in similar clinical indication (*9*). Until now ^{18}F-PSMA-1007 has not yet been benchmarked against other PSMA-ligands.

In this study an intra-individual comparison of ^{18}F-DCFPyL and ^{18}F-PSMA-1007 was performed.

MATERIALS AND METHODS

Patients

Twelve patients (median age 66 years, range: 54-82 years) suffering from newly diagnosed, treatment-naïve PCa were included in this study, which was approved by the Institutional Ethics Committee (University of Pretoria, South Africa), following written informed consent. Detailed patient characteristics are summarized in **Table 1**.

Radiopharmaceuticals

The radiolabeling precursors were obtained by ABX advanced biochemical compounds (Radeberg, Germany) in GMP-grade quality. ^{18}F-PSMA-1007 was produced on an automated radiosynthesizer (GE TRACERLab FX FN) in a one-step radiosynthesis (*10*) followed by a simple solid phase extraction cartridge separation of the product. The synthesis of ^{18}F-DCFPyL was performed as reported by Chen et al. (*5*). Analysis and quality control of the prepared products were realized as previously reported (*8*).

Imaging Procedures

Imaging was performed at two different days to minimize the effects of possible competitive interactions of the radiotracers. The first six patients were first imaged with ^{18}F-DCFPyL and 48 h later with ^{18}F-PSMA-1007. Then, another six patients were examined with ^{18}F-PSMA-1007 first, followed by a second examination with ^{18}F-DCFPyL 48 h later. Patients fasted for at least 4 h prior to injection of the radiotracer. For both tracers, the injected activities were 240-260 MBq and imaging was started 2 h post injection.

All scans were performed with a Biograph mCT 40 PET/CT scanner (Siemens, Erlangen,

Germany). For both tracers, a non-contrast-enhanced CT-scan was performed followed by PET-scans from thighs to the vertex. CT parameters were adjusted for patients' weight (120 KeV, 40-150 mAs) with a section width of 5mm and pitch of 0.8. Vertex to mid-thigh PET imaging was acquired in 3D mode at 3 minutes per bed position. Computed tomography data were used for attenuation correction. Image reconstruction was done with ordered subset expectation maximization iterative reconstruction algorithm (4 iterations, 8 subsets). A Gaussian filter was applied at 5.0 mm at full width at half maximum.

Image Analysis and Quantification

Clinical image interpretation was done independently by two board-approved nuclear medicine physicians with no case of disagreement in interpretation recorded. The two readers were blinded to findings on complementary imaging.

The tracer biodistribution was quantified by maximum standardized uptake value (SUV_{max}). Reconstructed images were displayed on a dedicated workstation equipped with syngo software (Siemens, Erlangen, Germany). A semi-automatic spherical volume of interest was drawn around lesions using a standardized uptake value threshold of 2.5 and a 3D isocontour of 41%. The volume of interest was manually adjusted to exclude areas of intense physiologic uptake contiguous to tumor. All primary tumors and up to 5 lymph nodes and 5 bone metastases, chosen by chance, were quantified. The normal bladder, background, brain, salivary and lacrimal glands, lung, liver, spleen, pancreas, small intestine, and kidneys were evaluated with a 2 cm sphere placed inside the organ parenchyma.

Statistical Analysis

Statistical analysis was performed using SPSS software, version 24.0 (IBM Corp., Armonk, NY). For comparison of uptake values, the nonparametric Wilcoxon signed-rank test for two related samples was used. The significance level used was $p \leq 0.05$ (two-tailed).

RESULTS

All subjects tolerated the examinations well and no drug-related adverse events occurred. The patients did not report any subjective symptoms. With regard to the clinical imaging interpretation both readers were concordant.

PSMA tracer-positive lesions were found in all patients. All lesions detected by ^{18}F-PSMA-1007 PET/CT were also detected by ^{18}F-DCFPyL PET/CT and vice versa. Seven patients presented with solitary tracer uptake in the prostate (**Figures 1 and 2**). One patient was diagnosed with prostate cancer and a single lymph node metastasis in the pelvis. In four patients, advanced metastatic disease was detected (**Figure 3**).

Tumor Uptake

There was no statistically significant difference found when evaluating uptake of ^{18}F-PSMA-1007 and ^{18}F-DCFPyL for local tumor growth (median SUV_{max}: 17.65 vs. 18.08, $p = 0.175$, n=12), lymph node metastases (median SUV_{max}: 13.97 vs. 17.33, $p = 0.109$, n = 17) and bone metastases (median SUV_{max}: 10.19 vs. 11.63, $p = 0.153$, n = 15). Detailed uptake characteristics for each lesion group are shown in **Figure 4**.

Normal-Organ Uptake

The biodistribution of both tracers differs as ^{18}F-DCFPyL presents with renal clearance and ^{18}F-PSMA-1007 is characterized by hepatobiliary clearance. There was a significantly higher uptake of ^{18}F-DCFPyL observed in the kidneys (median SUV_{max}: 37.50 vs. 22.08, $p < 0.001$), the urinary bladder (median SUV_{max}: 79.32 vs. 9.32, $p < 0.001$) and the lacrimal gland (median SUV_{max}: 8.37 vs. 7.30, $p = 0.036$) compared to ^{18}F-PSMA-1007. ^{18}F-PSMA-1007 presented with significantly higher uptake in liver (median SUV_{max}: 16.94 vs 9.07, $p < 0.001$), gallbladder (median SUV_{max}: 53.04 vs. 6.15, $p = 0.001$), spleen (median SUV_{max}: 14.32 vs. 6.68, $p < 0.001$), pancreas (median SUV_{max}: 4.55 vs. 2.95, $p = 0.003$), submandibular gland (median SUV_{max}: 17.39 vs. 13.20, $p = 0.011$), sublingual gland (median SUV_{max}: 3.97 vs. 3.30, $p = 0.006$) and muscle (median SUV_{max}: 1.10 vs. 0.97, $p = 0.034$). Tracer uptake did not differ significantly in fat tissue, blood pool (thoracic aorta), brain, nasal mucosa, parotid gland, lung or small intestine. Detailed comparison is shown in **Figure 4**.

DISCUSSION

In this intra-individual comparison of patients with treatment naïve PCa the diagnostic performance and tumor targeting of ^{18}F-DCFPyL and ^{18}F-PSMA-1007 were nearly identical. ^{18}F-DCFPyL is predominantly eliminated by renal clearance into the urinary bladder while ^{18}F-PSMA-1007 presents with hepatobiliary excretion characteristics.

Addressing the identical target structure, it is no surprise, that all PSMA-diagnostic agents, including the ^{68}Ga- (*11*) or ^{99m}Tc-labeled (*12*) compounds, present a similar specific accumulation in tumor and physiological PSMA-expressing normal organs, such as the healthy prostate, kidney parenchyma, salivary glands and the small intestine. ^{18}F-DCFPyL and ^{18}F-PSMA-1007 belong to the same family of PSMA-ligands based on the Glu-urea-Lys motif targeting the catalytic domain of PSMA and also share an aromatic portion considered to exploit the S1 hydrophobic accessory pocket close to the enzymatic binding site or the arene-binding site (*13*). Both tracers use the identical radiolabel ^{18}F, which based on its nuclear physical properties should allow equal or even improved spatial resolution than ^{68}Ga (*14*). Thus, comparable tumor targeting properties of these two evaluated ^{18}F-labeled tracers are reasonable and well addressed. In contrast, some differences can occur in the excretory organs. Vallabhajosula et al. already observed that structurally very similar PSMA-ligands can differ concerning hepatic (MIP-1404) or urinary (MIP-1405) excretion (*12*) and, due to rare hepatic metastases in prostate cancer, the MIP-1404 tracer with the lower bladder activity was chosen for phase-2/3 clinical trials (NCT0261506) (*15*). As local relapses are common and simultaneously a diagnostic challenge in the work-up of biochemical recurrence this rationale might also account for the ^{18}F-PSMA-1007 imaging findings.

Molecular size and excretion kinetics may also affect the velocity of tumor targeting and background clearance, which has relevant impact on the practicability of a particular tracer for

routine clinical use. For example, the dimerized form [Glu-ureido-Lys(Ahx)]$_2$-HBED-CC, named PSMA-10, presented with a higher PSMA binding affinity (IC_{50} 3.9 vs. 12.1 nM) compared with the monomer PSMA-11 (*16*), but due to the ability of early image acquisition the monomer became the standard tracer for imaging in combination with the short-lived radionuclide ^{68}Ga (*1*). Due to the longer half-life of ^{18}F, delayed imaging is possible using the radiofluorinated compounds. In particular, ^{18}F-PSMA-1007 demonstrated a remarkable increase of SUV when imaging was postponed until 3 h p.i. (*8*). In contrast, imaging 2 h p.i. was suggested for application of ^{18}F-DCFPyL by various groups (*7*,*9*). In this study, we decided to image 2 h p.i., as a physician's choice searching for a reasonable trade-off between contrast and optimal patient throughput in clinical practice.

The intra-individual comparisons are reasonable for this small patient population and highlight the potential benefit of each tracer's characteristics for the few patients with individually challenging situations. Larger comparison trials will be needed to validate the hypothesis that ^{18}F-PSMA-1007 might be advantageous for evaluation of the prostatic bed and ^{18}F-DCFPyL in the evaluation of liver metastases. No conclusion can be drawn from this study regarding the diagnostic performance of either tracer in imaging of prostate cancer as this was the aim of the study.

CONCLUSION

This study demonstrates that both ^{18}F-DCFPyL and ^{18}F-PSMA-1007 are widely equivalent for imaging of local and metastatic prostate cancer. Both tracers provide excellent image quality. As evaluation of the pelvis is more frequently the focus of PCa imaging than liver staging, the non-urinary excretion of ^{18}F-PSMA-1007 presents a theoretical advantage especially for primary staging and in case of suspected local recurrence.

DISCLOSURE

Conflict of Interests

Patent application for PSMA-1007 for FLG, KK and UH. The other authors declare that they have no conflict of interest.

ACKNOWLEDGEMENTS

Nuclear Technology Products (NTP), South African Nuclear Energy Corporation (NECSA) and Steve Biko Academic Hospital Nuclear Medicine Department. Daniel Burkert, Division of Radiopharmaceutical Chemistry, DKFZ Heidelberg, Germany for technical assistance with the radiosyntheses of ^{18}F-PSMA-1007 and ^{18}F-DCFPyL.

REFERENCES

1. Perera M, Papa N, Christidis D, et al. Sensitivity, specificity, and predictors of positive 68Ga-prostate-specific membrane antigen positron emission tomography in advanced prostate cancer: A Systematic Review and Meta-analysis. *Eur Urol.* 2016;70:926-937.

2. Kratochwil C, Afshar-Oromieh A, Kopka K, Haberkorn U, Giesel FL. Current status of prostate-specific membrane antigen targeting in nuclear medicine: Clinical translation of chelator containing prostate-specific membrane antigen ligands into diagnostics and therapy for prostate cancer. *Semin Nucl Med.* 2016;46:405-418.

3. Schwarzenböck SM, Rauscher I, Bluemel C, et al. PSMA ligands for PET-imaging of prostate cancer. *J Nucl Med.* July 7, 2017, doi: 10.2967/jnumed.117.191031.

4 Eiber M, Fendler WP, Rowe SP, et al. Prostate-specific membrane antigen ligands for imaging and therapy. *J Nucl Med.* 2017;58 (supplememt 2): 67S-76S.

5. Chen Y, Pullambhatla M, Foss CA, et al. 2-(3-{1-Carboxy-5-[(6-[18F]fluoro-pyridine-3-carbonyl)-amino]-pentyl}-ureido)-pen tanedioic acid, [18F]DCFPyL, a PSMA-based PET imaging agent for prostate cancer. *Clin Cancer Res.* 2011;17:7645-7653.

6. Cardinale J, Schafer M, Benesova M, et al. Preclinical evaluation of 18F-PSMA-1007, a new prostate-specific membrane antigen ligand for prostate cancer imaging. *J Nucl Med.* 2017;58:425-431.

7. Szabo Z, Mena E, Rowe SP, et al. Initial evaluation of [(18)F]DCFPyL for prostate-specific membrane antigen (PSMA)-targeted PET imaging of prostate cancer. *Mol Imaging Biol.* 2015;17:565-574.

8. Giesel FL, Hadaschik B, Cardinale J, et al. F-18 labelled PSMA-1007: biodistribution, radiation dosimetry and histopathological validation of tumor lesions in prostate cancer patients. *Eur J Nucl Med Mol Imaging.* 2017;44:678-688.

9. Dietlein F, Kobe C, Neubauer S, et al. PSA-Stratified performance of 18F- and 68Ga-PSMA PET in patients with biochemical recurrence of prostate cancer. *J Nucl Med.* 2017;58:947-952.

10. Cardinale J, Martin R, Remde Y, et al. Procedures for the GMP-compliant production and quality control of [18F]PSMA-1007: A next generation radiofluorinated tracer for the detection of prostate cancer. *Pharmaceuticals (Basel).* 2017;10:77. doi:10.3390/ph10040077.

11. Afshar-Oromieh A, Malcher A, Eder M, et al. PET imaging with a [68Ga]gallium-labelled PSMA ligand for the diagnosis of prostate cancer: biodistribution in humans and first evaluation of tumour lesions. *Eur J Nucl Med Mol Imaging.* 2013;40:486-495.

12. Vallabhajosula S, Nikolopoulou A, Babich JW, et al. 99mTc-labeled small-molecule inhibitors of prostate-specific membrane antigen: pharmacokinetics and biodistribution studies in healthy subjects and patients with metastatic prostate cancer. *J Nucl Med.* 2014;55:1791-1798.

13. Kopka K, Benesova M, Barinka C, Haberkorn U, Babich J. Glu-Ureido-based inhibitors of prostate-specific membrane antigen: Lessons learned during the development of a novel class of low-molecular-weight theranostic radiotracers. *J Nucl Med.* 2017;58:17s-26s.

14. Sanchez-Crespo A. Comparison of Gallium-68 and Fluorine-18 imaging characteristics in positron emission tomography. *Appl Radiat Isot.* 2013;76:55-62.

15. Goffin KE, Joniau S, Tenke P, et al. Phase 2 study of 99mTc-Trofolastat SPECT/CT to identify and localize prostate cancer in intermediate- and high-risk patients undergoing radical prostatectomy and extended pelvic LN dissection. *J Nucl Med.* 2017;58:1408-1413.

16. Schafer M, Bauder-Wust U, Leotta K, et al. A dimerized urea-based inhibitor of the prostate-specific membrane antigen for 68Ga-PET imaging of prostate cancer. *EJNMMI Res.* 2012;2:23.

TABLES

TABLE 1 – Patient characteristics.

Patient no.	Age [y]	Gleason Score	PSA at examination [ng/mL]	Local tumor growth	Lymph node metastases	Bone metastases
1	54	9 (4+5)	124.0	1	>10	>10
2	55	8 (4+4)	112.0	1	0	0
3	60	6 (3+3)	13.4	1	0	0
4	66	8 (4+4)	75.0	1	>10	4
5	80	8 (4+4)	95.4	1	0	0
6	82	9 (5+4)	240.0	1	>10	>10
7	66	7b (4+3)	87.0	3	0	0
8	66	7a (3+4)	61.6	1	0	0
9	69	7a (3+4)	10.0	2	0	0
10	62	7b (4+3)	83.0	1	1	0
11	79	8 (4+4)	279.8	1	>10	0
12	65	7 (3+4)	55.2	1	0	0

FIGURES

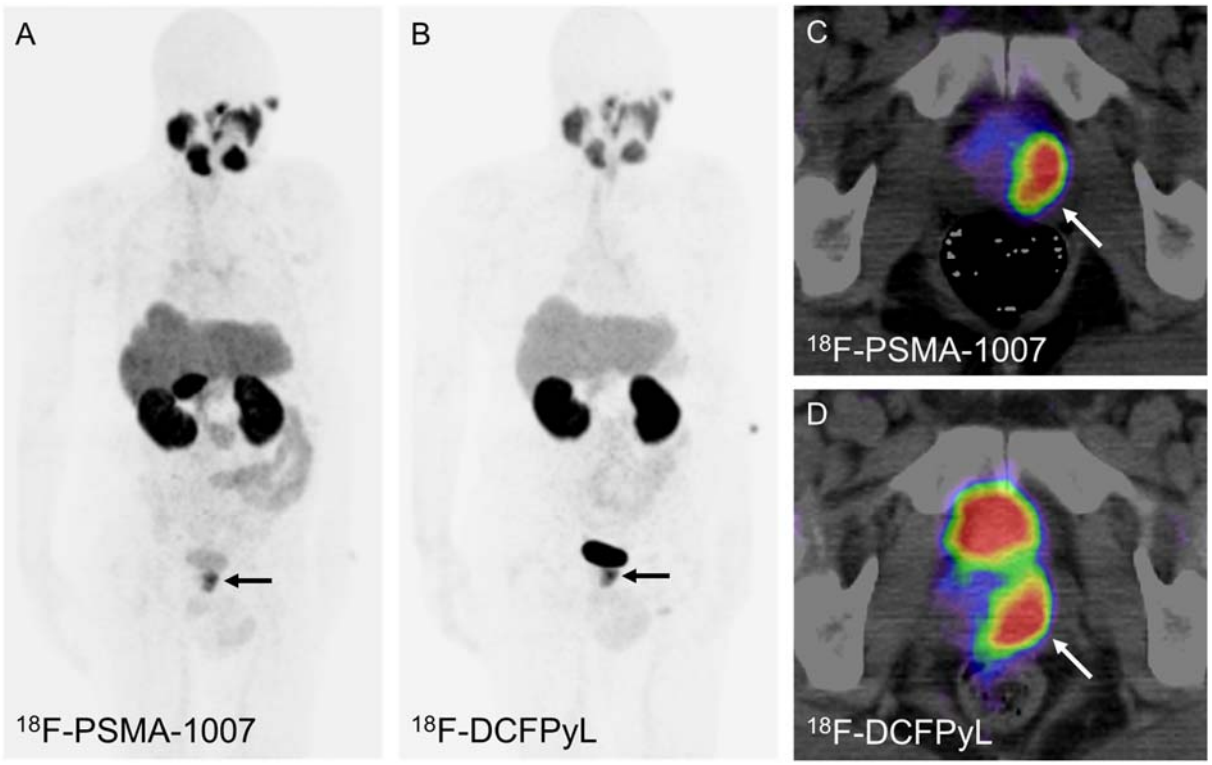

FIGURE 1 – An 80-year old patient with newly diagnosed prostate cancer was referred to the institution due to a PSA serum-level of 95.43 ng/mL and positive biopsy (Gleason score 8 (4+4)). This patient was examined with ^{18}F-DCFPyL (B, D) in May 2017. A second examination with ^{18}F-PSMA-1007 followed 48 h thereafter (A, C). The diagnosis of prostate cancer confined to the prostate gland (arrow) was possible with both tracers. SUV_{max} in this lesion were 18.08 and 11.77 for ^{18}F-DCFPyL and ^{18}F-PSMA-1007, respectively.

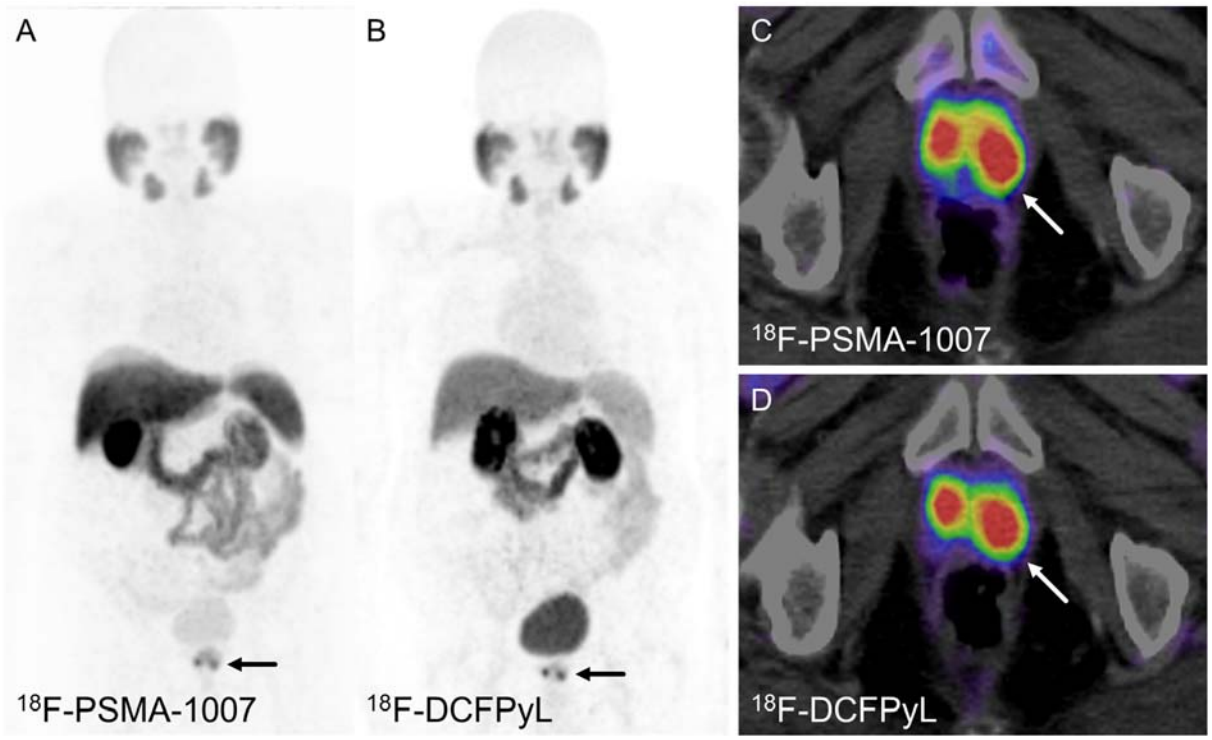

FIGURE 2 – This image shows ^{18}F-PSMA-1007 (A, C) and ^{18}F-DCFPyL (B, D) examinations of a 65-year old patient who was referred to the institution with a Gleason score of 7a (3+4) and a PSA serum-level of 55.2 ng/mL. PET/CT imaging showed bifocal prostate cancer (arrow). Delineation of tumor growth in both lobes of the prostate was possible with both tracers. SUV_{max} values were 17.68 and 19.65 in the right lobe and 14.21 and 16.60 in the left lobe for ^{18}F-DCFPyL and ^{18}F-PSMA-1007, respectively.

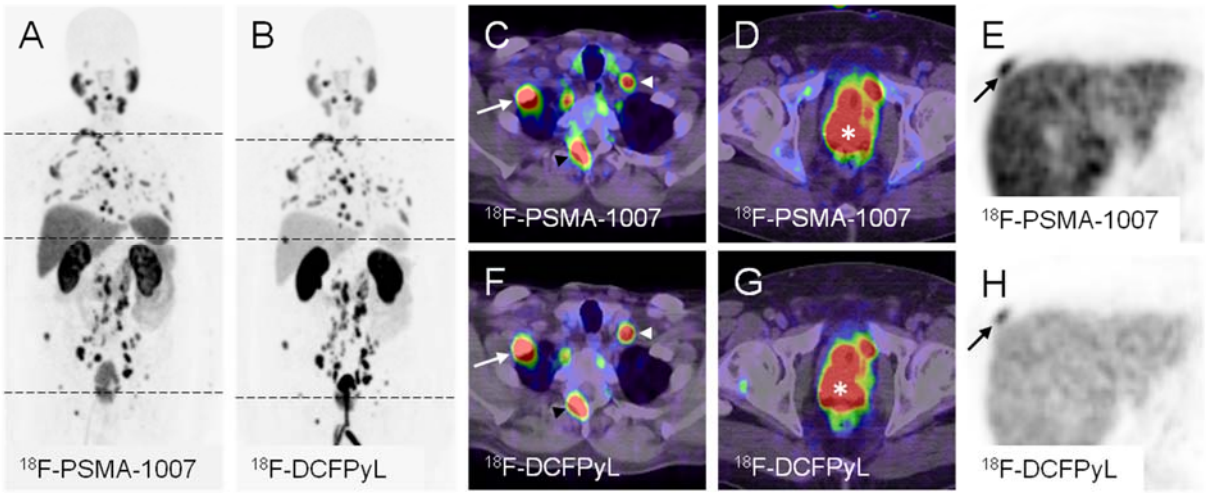

FIGURE 3 – The image shows maximum intensity projections of PET examinations using ^{18}F-PSMA-1007 (A) and ^{18}F-DCFPyL (B) as well as exemplary cross-sections with bone and lymph node metastases (C, E, F, H) and local tumor (D, G). The 82-year old patient presented with a PSA serum-level of 240.0 ng/mL at the time of the examinations. The subject was diagnosed with highly-advanced metastatic prostate cancer (Gleason 9 (5+4)) and was treatment-naïve at the time of the examinations. The SUV_{max} values were 22.80 and 19.69 in the prostate (D, G, asterisk), 16.50 and 11.20 in an exemplary lymph node (C, F, white arrowhead) and 16.20 and 13.72 (C, F, white arrow) and 25.45 and 24.90 (A, D, black arrowhead) in exemplary bone lesions for ^{18}F-DCFPyL and ^{18}F-PSMA-1007, respectively. The maximum intensity projections (A, B) demonstrate a bone lesion that could be missed on the ^{18}F-PSMA-1007 maximum intensity projection (A). However, it is delineable on transaxial cross-sections (E, H, black arrow). This lesion presents with SUV_{max} values of 23.72 and 17.97 for ^{18}F-DCFPyL and ^{18}F-PSMA-1007, respectively. This case highlights the differences in biodistribution of the tracers and similar uptake in all tumor lesions. A urinary catheter is also seen.

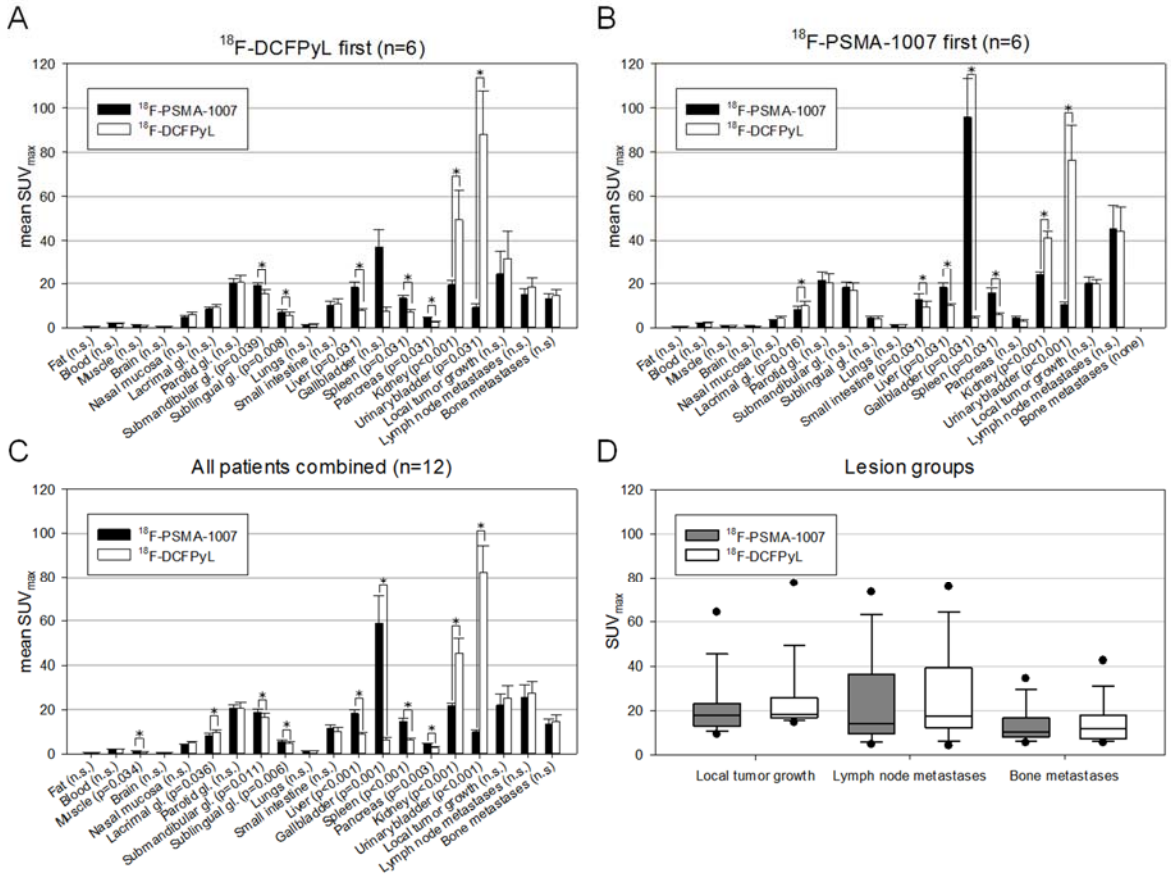

FIGURE 4 – A: Comparison of mean SUV_{max} and its standard error 2 hours after injection of ^{18}F-PSMA-1007 and ^{18}F-DCFPyL for normal organs and tumor lesion groups in the six patients that were examined with ^{18}F-DCFPyL prior to being examined with ^{18}F-PSMA-1007 is shown. If significance was observed, differences are marked with (*) and *p*-values are given. **B:** Comparison of mean SUV_{max} and its standard error 2 hours after injection of ^{18}F-PSMA-1007 and ^{18}F-DCFPyL for normal organs and tumor lesion groups in the six patients that were examined with ^{18}F-PSMA-1007 prior to being examined with ^{18}F-DCFPyL is shown. Statistical significance is highlighted as described above. **C:** Comparison of mean SUV_{max} and its standard error 2 hours after injection of ^{18}F-PSMA-1007 and ^{18}F-DCFPyL for normal organs and tumor lesion groups in all patients is shown. Statistical significance is highlighted as described above. **D:** Box plots showing SUV_{max}

for ^{18}F-PSMA-1007- and ^{18}F-DCFPyL-positive lesions. There were no significant differences observed.